

Hydrogenated polystyrene–poly(methyl methacrylate) diblock copolymer micelles in selective solvent: 2. Binary solvent–precipitant mixtures – effect of mixture composition and temperature

Michel Duval and Claude Picot

*Institut Charles Sadron (CRM-EAHP), CNRS-ULP, 6 rue Boussingault, 67083
Strasbourg, France*

(Received 8 April 1986; revised 8 September 1986; accepted 12 September 1986)

The association of a polystyrene–poly(methyl methacrylate) (PS–PMMA) diblock copolymer in 1-chloro-*n*-hexane/dioxane mixture has been studied by light scattering. A parallel is made between the effect of the addition of precipitant for one block and the decrease of the temperature. As the volume fraction ϕ of precipitant for the PMMA block increases, or at constant ϕ as the temperature T decreases, multimolecular aggregation occurs. Contrary to the degree of association of the molecules, which varies, the dimensions of the micelles are independent of ϕ or T so that the compactness of those micelles increases when ϕ increases or T decreases. At intermediate T or ϕ values, large structures seem to be present in dilute solution.

(Keywords: diblock copolymer; polystyrene–poly(methyl methacrylate); integrated light scattering; quasi-elastic light scattering; micelle)

INTRODUCTION

In a previous paper¹ the influence of a selective solvent on the formation of micellar structures by diblock copolymers in dilute solution has been investigated where the quality of the solvent was controlled by the temperature. Large multimolecular aggregates have been characterized in a temperature range around the theta temperature for one component of the diblock copolymer and good solvent for the other. Compact micelles have been observed below this range of temperature. The core of the micelle, which is very dense, is formed by the insoluble sequence of the copolymer surrounded by the soluble part. In this micellar structure the degree of association of macromolecules is greatly dependent on the temperature. The results obtained were in good agreement with the model of 'closed association' proposed by Elias².

In the present study and in a first stage, starting with dilute solutions of a polystyrene–poly(methyl methacrylate) (PS–PMMA) diblock copolymer in good solvent for the two components of the copolymer, the thermodynamic quality of the solvent has been modified by addition of precipitant at room temperature. Micellar structures are observed after addition of a certain volume fraction of precipitant for PMMA blocks. This behaviour of the diblock copolymer is compared to the behaviour in single solvent.

In a second stage of the study, a much more detailed analysis of the process of micellization has been carried out by variation of the temperature in the vicinity of this characteristic volume fraction of precipitant.

The molecular weight M and the second virial coefficient A_2 of the micelles have been measured by conventional integrated light scattering (ILS) measure-

ments. Unfortunately their dimensions were not large enough to be measured accurately by this method. On the other hand, quasi-elastic light scattering (QELS) experiments, which are very sensitive to the dimensions and to the polydispersity of the scattering particles, have been used to follow the variation of the dimensions of the particles as a function of the volume fraction of the precipitant or as a function of the temperature.

Finally, in the concluding part of this paper and through the results obtained here and in the previous paper¹, we compare the behaviour of diblock copolymers in solution when the quality of the solvent towards one block is changed either by variation of the temperature or by addition of precipitant.

EXPERIMENTAL

Materials

For the purpose of comparison, the copolymer/selective solvent system used in the present study is identical to the system investigated in the previous study¹, where the molecular characteristics of the PSH47-PMMA22 are given.

PMMA homopolymers precipitate at 92°C in 1-chloro-*n*-hexane, which is the selective solvent. In this study, dioxane, a good solvent of PMMA and PS, is chosen as good solvent for the diblock copolymer. Moreover, dioxane is miscible with 1-chloro-*n*-hexane and has the same refractive index. Thus dioxane/1-chloro-*n*-hexane seems to be a very suitable binary system for light scattering investigation. The interpretation of the results is simplified because the effect of preferential solvation can be neglected³.

Photon correlation spectroscopy

QELS measurements were performed with a home-built 'software correlator'. A monochromatic incident beam from a Spectra Physics model 165 argon-ion laser was polarized perpendicularly to the scattering plane. The laser was operated at a wavelength $\lambda_0 = 488$ nm and in the optical stabilization mode. The optical and mechanical parts of the experimental set-up have been described previously⁴. The scattered signal going through a photon counting system is sent to a minicomputer (DEC-PDP 11/34) in a real-time experiment.

The full homodyne correlation function, defined on 100 channels, was calculated and accumulated in the computer. The software treatment of the data and the analysis of the experimental curves using a routine least-squares exponential fit are described elsewhere⁵.

For a monodisperse polymer sample in dilute solution, the experimental correlation function of the scattered intensity fits an exponential curve:

$$G(t) = A \exp(-\Gamma t) + B \quad (1)$$

where t is the time delay and A and B are constants. The translational diffusion coefficient D of the scattering particles was calculated from:

$$\Gamma = 2Dq^2 \quad (2)$$

where q is the wavevector:

$$q = (4\pi/\lambda_0)n \sin(\theta/2) \quad (3)$$

In equation (3), n is the refractive index of the solvent, θ is the scattering angle and λ_0 the wavelength of the incident light in vacuum.

Dilute solutions of low molecular weight samples are characterized by low light scattering levels and fast motions. Thus the smallest available angle ($\theta = 20^\circ$) was selected for all the measurements. Nevertheless, the relation between Γ and q^2 (relation (2)) was checked for strongly scattering solutions (study at high volume fraction of precipitant or low temperature).

The concentration dependence of D was analysed and a translational diffusion coefficient D_0 extrapolated to zero concentration was deduced through the relation:

$$D = D_0(1 + k_D c) \quad (4)$$

where k_D is the dynamic second virial coefficient and c is expressed in g g^{-1} .

From the D_0 values, the hydrodynamic radii R_H of the scattering particles were calculated using the well known Stokes-Einstein relation for diffusion:

$$R_H = \frac{k_B T}{6\pi\eta_0 D_0} \quad (5)$$

where k_B is the Boltzmann constant, T the absolute temperature and η_0 the viscosity of the solvent. The viscosity of the dioxane/1-chloro-n-hexane mixture has been measured at several volume fractions ϕ of 1-chloro-n-hexane taking account of the density of the mixture.

RESULTS AND DISCUSSION

Effect of mixture composition ($T = 25^\circ\text{C}$)

ILS experimental results. On Figure 1 are shown the variations of the reduced scattered light intensity (c/I) by copolymer solutions at several volume fractions ϕ of 1-

chloro-n-hexane as a function of the polymer concentration c . This variation is linear for ϕ values less than or equal to 0.80. In this domain the slopes of c/I versus c decrease with increasing ϕ but the extrapolated values of c/I at zero concentration remain constant.

At ϕ values between 0.80 and 0.90 there is an extensive increase of the scattered light which is no longer a linear function of c at least in the range of concentration investigated. At higher ϕ values the plots are linear and quasi-independent of the concentration but the extrapolated values of c/I at $c = 0$ are considerably lower than those obtained in the low ϕ range.

On Figure 2 are plotted the M and A_2 values calculated respectively from the extrapolation to zero concentration and from the slopes of the plots drawn on Figure 1 as a function of ϕ .

In the first domain ($0 < \phi < 0.90$) the molecular weight of the scattering particles does not vary and is equal to the molecular weight of a single copolymer molecule. Meanwhile, in this ϕ range, the A_2 values decrease to negative values as a consequence of the decreasing quality of the solvent by addition of precipitant.

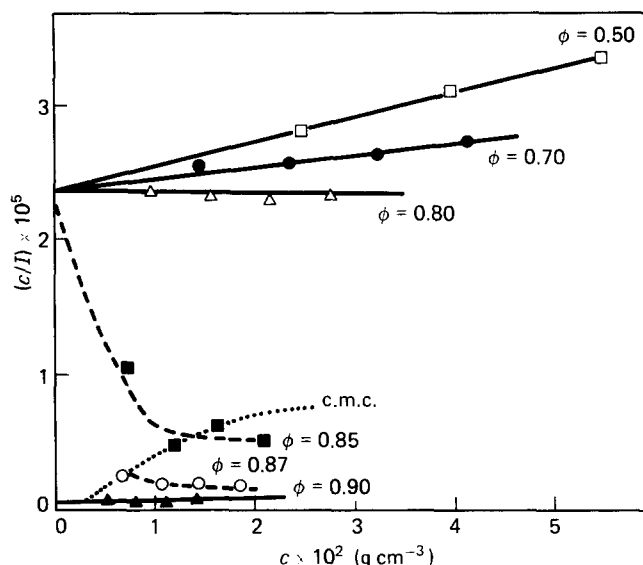


Figure 1 Concentration dependence of c/I (arb. units) at scattering angle of 90° , for various ϕ (volume fraction of 1-chloro-n-hexane) ($T = 25^\circ\text{C}$): --- schematic interpolation; schematic variation of the c.m.c.

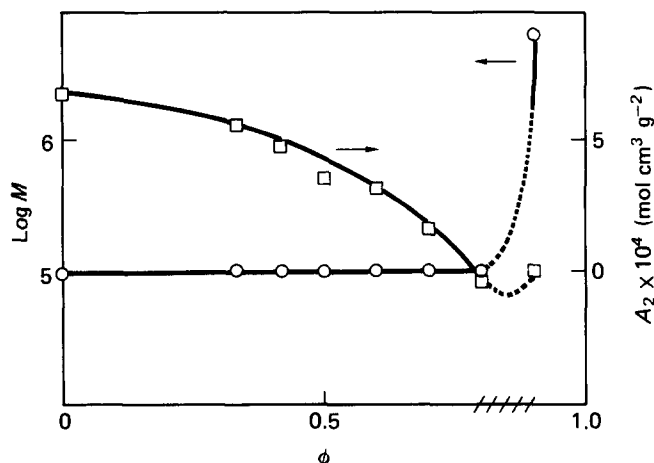


Figure 2 Variation of the molecular weight (\circ) and second virial coefficient (\square) as a function of ϕ ($T = 25^\circ\text{C}$): schematic interpolation; dashed lines represent domain of non-linear Zimm plot

At $\phi = 0.90$ the molecular weight of the scattering particles, as given by light scattering, is $6.1 \times 10^6 \text{ g mol}^{-1}$, which corresponds to the association of about 60 molecules. At this ϕ value, A_2 is very low but positive ($A_2 = 6 \times 10^{-6} \text{ cm}^3 \text{ g}^{-2} \text{ mol}$) and the Zimm plot does not allow a radius of gyration to be calculated. Copolymer molecules are associated according to a compact micellar structure.

The dashed domain on Figure 2 ($0.80 < \phi < 0.90$) is not well defined. In this domain the Zimm plots are non-linear and no M or A_2 values could be extracted.

QELS experimental results. On Figure 3 are plotted the variations of the translational diffusion coefficient D at several ϕ values as a function of the copolymer concentration. As for static light scattering experiments, three domains can be distinguished.

As the selective solvent is added, for ϕ lower than or equal to 0.60, the plots are linear. The slopes of these plots are positive and decrease as ϕ increases. The viscosity of the binary solvent is lowered as the ϕ values become higher. This results in a decrease of the extrapolation of D to zero concentration.

For $0.60 < \phi < 0.90$, besides small fluctuations of the scattered intensities as a function of time, large fluctuations can be observed and no single relaxation time of the correlation function can be calculated.

At $\phi = 0.90$ the correlation function of the scattered intensity is monoexponential for all the concentrations and the D versus c variation is linear and exhibits a very slight slope.

On Figure 4 are plotted the variations of the hydrodynamic radius R_H and dynamic second virial coefficient k_D as a function of ϕ .

At $\phi < 0.60$, R_H is low ($R_H = 7.5 \text{ nm}$) and independent of ϕ . The constant k_D is positive but decreases with increasing ϕ . The copolymer molecules are unassociated and addition of precipitant decreases the quality of the solvent.

At $\phi = 0.90$, R_H has increased ($R_H = 34 \text{ nm}$) and k_D is very low but still positive.

There is a large ϕ range ($0.60 < \phi < 0.90$; dashed region on Figure 4) which corresponds to multiexponential correlation functions of the scattered light.

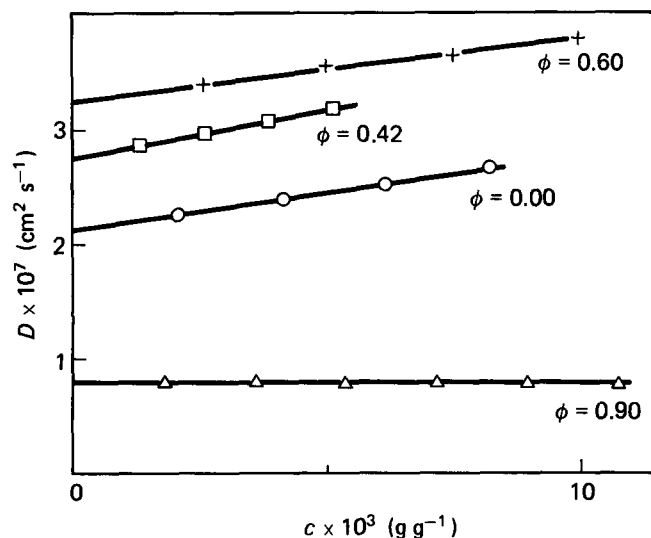


Figure 3 Concentration dependence of the translational diffusion coefficient at several ϕ ($T = 25^\circ\text{C}$)

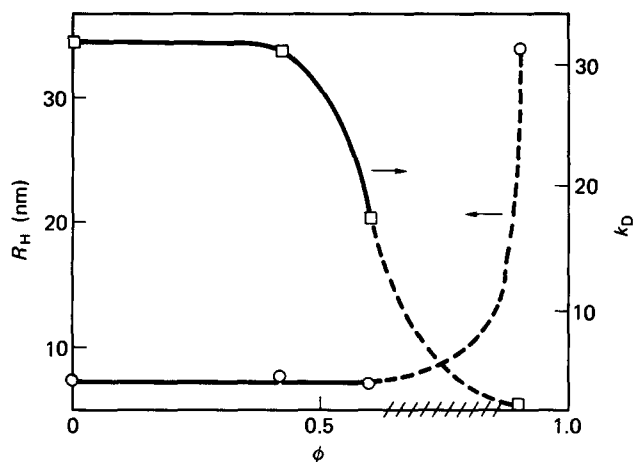
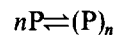


Figure 4 Variation of the hydrodynamic radius (O) and dynamic virial coefficient (□) as a function of ϕ ($T = 25^\circ\text{C}$): --- schematic interpolation; dashed lines represent domain of multiexponential correlation functions of the scattered intensity

Discussion. The pattern of the experimental curves shown on Figure 1, particularly in the intermediate ϕ range ($0.80 < \phi < 0.90$), agrees well with the closed association model proposed by Elias². In this domain and in the lowest concentration range, up to a concentration that can be named the critical micelle concentration (c.m.c.), only monomers are present in the solution.

In the middle range of polymer concentration, the equilibrium



between monomer and micelle shifts towards micelle with increasing concentration. At higher concentration the solution contains practically only multimolecular micelles. On Figure 1 an approximate curve has been drawn which represents the variation of the c.m.c. with ϕ . Unfortunately this c.m.c. value is poorly defined and depends on the type of experiment used to study the copolymer solutions⁶. Nevertheless it decreases strongly with worsening of the thermodynamic conditions of the insoluble copolymer sequence.

The QELS results are comparable with those obtained for other copolymer/solvent-non-solvent systems^{7,8}. The hydrodynamic dimensions in the micellar state are higher than in the unassociated state, but remain small with respect to the high molecular weight of the micelles. This small value of R_H is consistent with the small value of the dissymetry of the scattered light observed by ILS. However, it should be noted that the correlation functions of the scattered intensity are no longer exponential in the range $0.60 < \phi < 0.90$ while the inverse of the scattered intensity is linear with c only for $0.80 < \phi < 0.90$. This fact can be ascribed to the higher sensitivity of the QELS technique. This suggests that it should be possible to observe by QELS the collapse of the PMMA subchain in the monomer state before multimolecular association. In fact, in the small ϕ range involved ($\phi \sim 0.60$) this effect is strongly screened by the multimolecular aggregation effect. Tentatively a subsequent careful mathematical treatment of the experimental data, obtained on more dilute solutions in this ϕ range, could lead to the observation of such monomolecular micelles⁹.

Effect of temperature variation ($\phi=0.90$)

As mentioned in the previous section, PSH47-PMMA22 diblock copolymer in dioxane/1-chloro-n-hexane (10/90) solution exhibits micellar aggregates at room temperature in the whole range of concentration investigated ($1.5 \times 10^{-3} \text{ g cm}^{-3} < c < 9 \times 10^{-3} \text{ g cm}^{-3}$). Thus it was of interest to modify the equilibrium of the system by temperature effect and to characterize the resulting molecular species.

ILS experimental results. On Figure 5 are plotted the variations of the inverse of the scattered intensity as a function of the polymer concentration.

At low ($T < 24^\circ\text{C}$) and high ($T \geq 62.7^\circ\text{C}$) temperatures the plots are linear with positive slopes. The intercept, at zero concentration, is raised by a factor of 10 when the temperature increases.

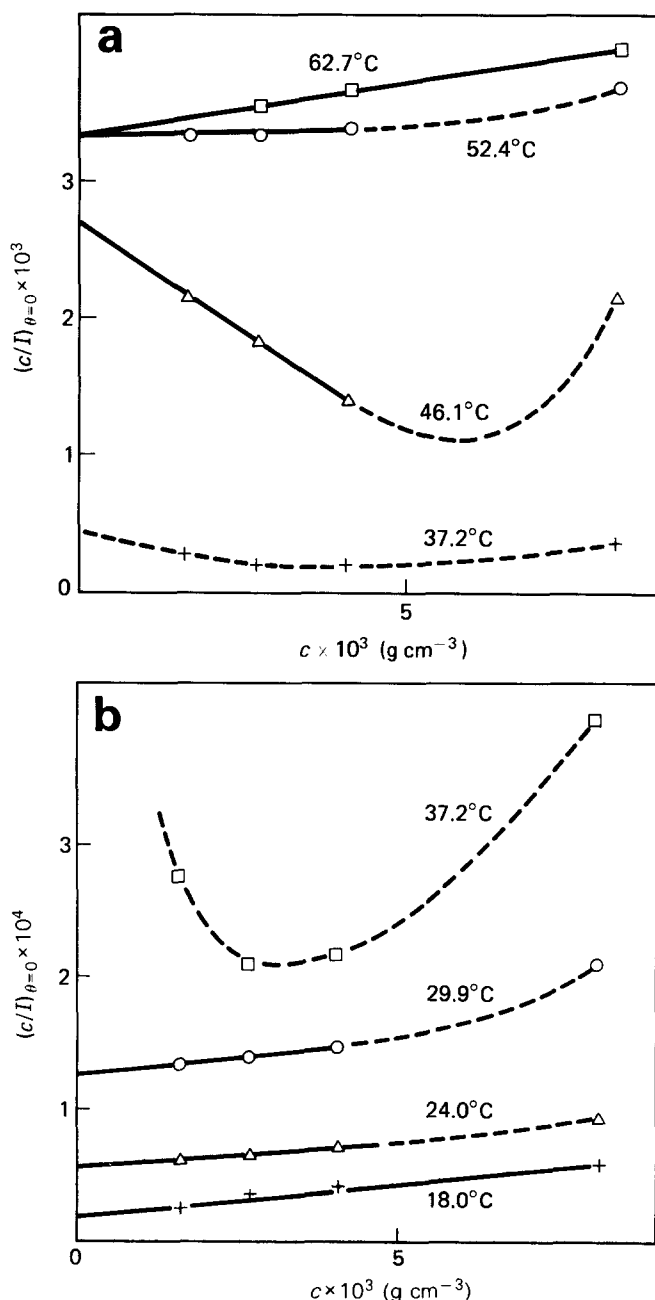


Figure 5 Concentration dependence of c/I extrapolated to zero scattering angle at several temperatures ($\phi=0.90$): --- schematic interpolation

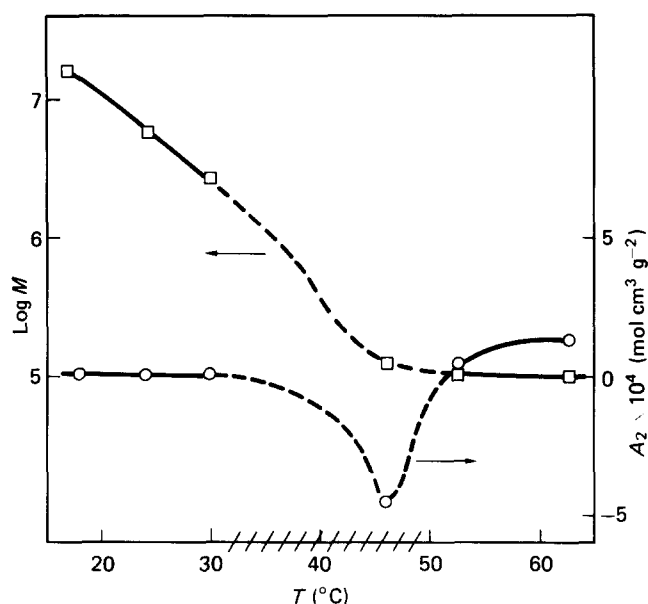


Figure 6 Temperature dependence of the molecular weight and second virial coefficient ($\phi=0.90$): --- schematic interpolation; dashed lines represent domain of non-linear Zimm plot

Between 24 and 62.7°C no linear variation of $c/I=f(c)$ can be observed. Then, it is suitable to define a range of concentration which depends on the temperature where linear variation still occurs.

On Figure 6 are plotted the variations of A_2 and $\log_{10} M$ as a function of the temperature where A_2 and M are respectively calculated from the slope and the extrapolation to zero concentration of the linear parts of the plots in Figures 5a and 5b. Three temperature domains can be defined from this figure.

At high temperature ($T > 50^\circ\text{C}$) the molecular weight of the scattering particles remains constant and equal to the molecular weight of the isolated diblock copolymer as measured in dioxane solution for example (Figure 2). Meanwhile A_2 decreases when the temperature decreases.

Between 50 and 30°C (dashed domain on Figure 6) the Zimm plots are non-linear in the range of concentration investigated and only approximate A_2 or M values can be calculated from the initial linear behaviour of $c/I=f(c)$.

Below 30°C the mass of the scattering particles increases with subsequent decreasing temperature while A_2 remains constant with small positive values. Stable multimolecular micelles are formed.

QELS experimental results. On Figure 7 are plotted the variations of the inverse of the relaxation time Γ which characterizes the correlation function of the scattered light as a function of the square of the wavevector at several temperatures. These plots are linear according to relation (2) for all the concentrations investigated. The intensity of the light scattered by the copolymer solutions is very weak at high temperatures ($T > 47.2^\circ\text{C}$). For such experimental conditions, QELS measurements were made at $\theta = 20^\circ$ only.

The variation of the translational diffusion coefficient D as a function of the polymer concentration c is represented on Figure 8.

At high ($T = 59.8^\circ\text{C}$) and low ($T < 26^\circ\text{C}$) temperatures, the variations are linear. In the intermediate temperature range, relation (4) does not hold over the whole range of polymer concentrations investigated. However, the

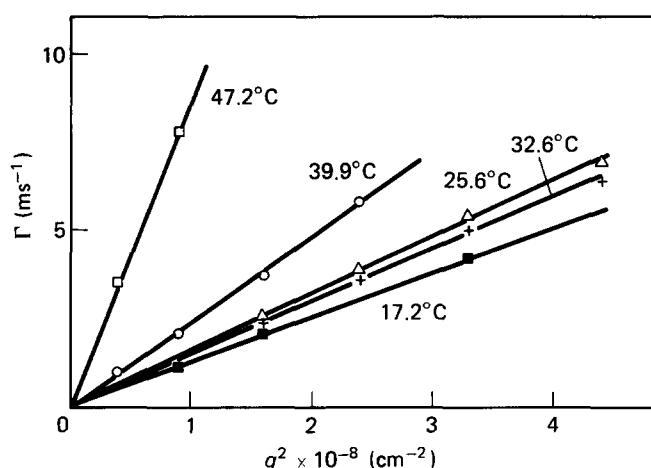


Figure 7 The q^2 dependence of the inverse of the relaxation time of the correlation function of the scattered intensity at the temperatures indicated ($\phi=0.90$; $c=1.79 \times 10^{-3} \text{ g g}^{-1}$)

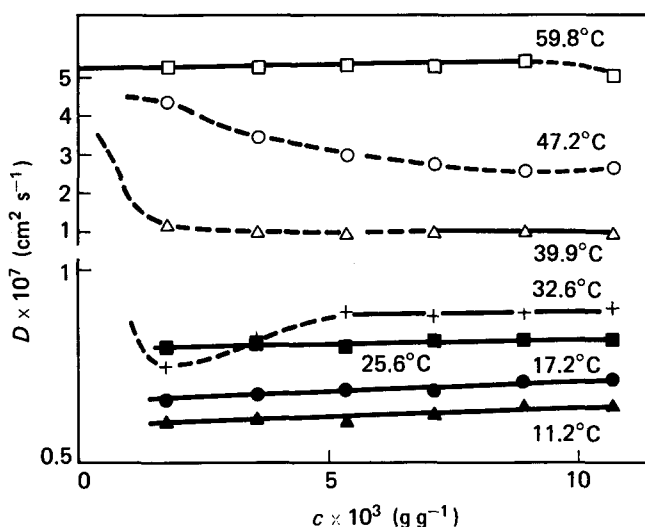


Figure 8 Concentration dependence of the translational diffusion coefficient at the temperatures indicated ($\phi=0.90$): --- schematic interpolation; — linear fit with the experimental points

correlation functions remain monoexponential despite the fact that the adjustment parameters are not as satisfactory as in the high- or low-temperature regions (for example the alternance parameter⁵ Q is lower than 0.70).

On Figure 9 are plotted the R_H and k_D variations as a function of the temperature. Three regions can still be distinguished.

At high temperature, R_H is low (7.5 nm) and k_D positive ($k_D=4$) according to the values for equivalent homopolymer in good solvent.

At low temperature ($T < 40^\circ\text{C}$), R_H is constant ($R_H \sim 34.5 \text{ nm}$) while k_D goes from negative to positive values when T decreases.

In the intermediate temperature range, as seen previously, D is not linear with c and R_H or k_D values cannot be calculated from equations (4) and (5). This region corresponds to the dashed region in Figure 9.

Discussion. As in the first part of this paper, static (see Figure 5) and dynamic (Figure 8) results can be interpreted in the frame of the model of closed association of diblock copolymer molecules where the equilibrium between unimer and plurimer is shifted towards plurimer formation as the temperature decreases.

In the two kinds of experiments involved in this study (ILS and QELS), an equivalent domain of temperature can be defined between 50 and 25°C where there is no linear variation of c/I or D as a function of c in the whole concentration range. In this concentration range, by analogy with a c.m.c., a critical micelle temperature¹⁰ (c.m.t.) could be defined.

In contrast, well defined entities contribute to the scattering at high or low temperatures (Figure 6 for static and Figure 9 for dynamic results). At high temperature ($T > 50^\circ\text{C}$), unimers ($M=10^5 \text{ g mol}^{-1}$) with small hydrodynamic radius ($R_H \sim 7.5 \text{ nm}$) are present in the medium. Dynamic and static virial coefficients decrease when the temperature is decreased. At low temperature ($T < 26^\circ\text{C}$) micelles are formed with increasing molecular weight but constant hydrodynamic radius as the temperature decreases. Very weak repulsive interactions take place between those micelles (k_D , $A_2 \sim 0$). In this temperature range, the lower the temperature, the more compact are the micelles.

Finally it must be pointed out that, in the temperature range where $D(c)$ does not exhibit a linear behaviour and where monomolecular micelles could be formed by collapse of the PMMA sequences, no such species could be identified.

CONCLUSIONS

The results of light scattering and photon correlation spectroscopy on solutions of polystyrene-poly(methyl methacrylate) copolymer in 1-chloro-*n*-hexane/dioxane mixtures are in qualitative agreement with those obtained in single selective solvent¹ at least in the limiting cases of high ϕ or low T values. For example, Figure 3 in the first study¹ can be compared directly to Figures 2 and 6 in the present work. The complementarity of the ϕ or T variation (last part in this paper) allows a progressive description of the behaviour of the diblock copolymer as the thermodynamic parameters are modified (compare Figures 4 and 9 of this study). Moreover, all the measurements on the micellar solutions are reproducible and physical parameters such as M or R_H are independent of the thermal history of the solutions.

At high temperatures (not reached in the first paper at $\phi=1$, but for $T > 52^\circ\text{C}$ at $\phi=0.90$) or low weight fractions of precipitant ($\phi < 0.80$ at room temperature),

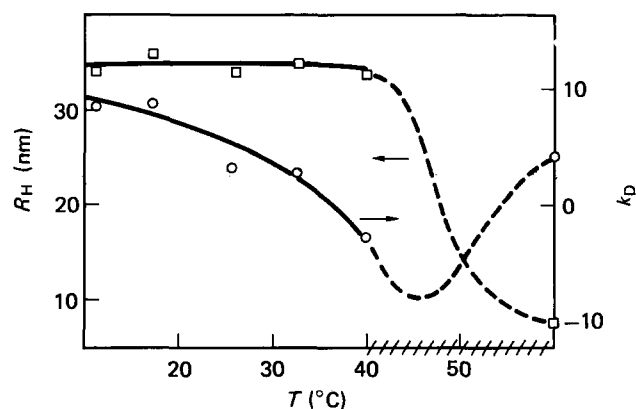


Figure 9 Temperature dependence of the hydrodynamic radius (\square) and dynamic virial coefficient (\circ) ($\phi=0.90$): --- schematic interpolation; dashed lines represent temperature range of non-linearity of $D=f(c)$ plot (see Figure 8)

only unassociated diblock copolymer molecules are present in the solution.

At low temperature ($T < 30^\circ\text{C}$) or high weight fractions of precipitant ($\phi > 0.90$), micelles are preponderant, although a small amount of unassociated molecules must still remain in the solution as shown by ultracentrifugation measurements. Thus quantitative study is made complicated and a careful evaluation of the M or R_H parameters would be required to determine the contributions of the different species to the scattered intensity. Yet, in this range of ϕ or T , the light is mainly scattered by heavy, large micelles. ILS measurements could not provide any information on the radii of gyration of the micelles, since no angular dependence of the intensity of the scattered light has been observed. Nevertheless, translational diffusion coefficients were obtained from the autocorrelation functions by a perfect single-exponential fit. This demonstrates that the micelles are very monodisperse in size with constant dimensions as T or ϕ are changed ($R_H = 35\text{ nm}$). The same conclusion does not hold for the molecular weight or the degree of association of the particles, since M increases with worsening of the thermodynamic conditions. Also, the micelles become more and more compact, as was confirmed in the first paper by neutron scattering. Finally it should be noted that, in this T or ϕ range, the thermodynamic and hydrodynamic interactions between micelles are very weak as shown by the low A_2 and k_D values.

In the intermediate temperature range ($T > 30^\circ\text{C}$ at $\phi = 1$ or $30^\circ\text{C} < T < 50^\circ\text{C}$ at $\phi = 0.90$) or at intermediate weight fractions of precipitant ($0.60 < \phi < 0.90$ at room temperature) the behaviour of the copolymer solutions is more complex. In addition to T and ϕ , their properties are strongly dependent on the concentration of the copolymer. At very low or high copolymer concentration, the situation is similar to, respectively, homopolymer dilute solutions or micellar solutions already described. The limits of this range of concentration are not well defined. The lower borderline could be called the critical micelle concentration (c.m.c.) or the critical micelle temperature (c.m.t.) limit. In this frame all the previously plotted curves (previous¹ and present paper) could be plotted as universal curves as a function of reduced standard variables such as $(c - \text{c.m.c.})/\text{c.m.c.}$ or $(T - \text{c.m.t.})/\text{c.m.t.}$. Figure 10 shows the schematic behaviour of such a universal curve where the ordinate could represent the inverse of the scattered intensity or the translational diffusion coefficient at a given concentration.

The region 2, on this plot, corresponds to the so-called 'anomalous micellization effect' observed in some other micellar systems¹⁰⁻¹². This schematic curve can be compared directly to the experimental curves of Figure 8 shifted towards the low concentration range when the temperature is raised from 32.6 to 59.8°C (dynamic results). It can also be compared to the curves of Figures 5a and 5b when the temperature is raised from 29.9 to 52.4°C (static results).

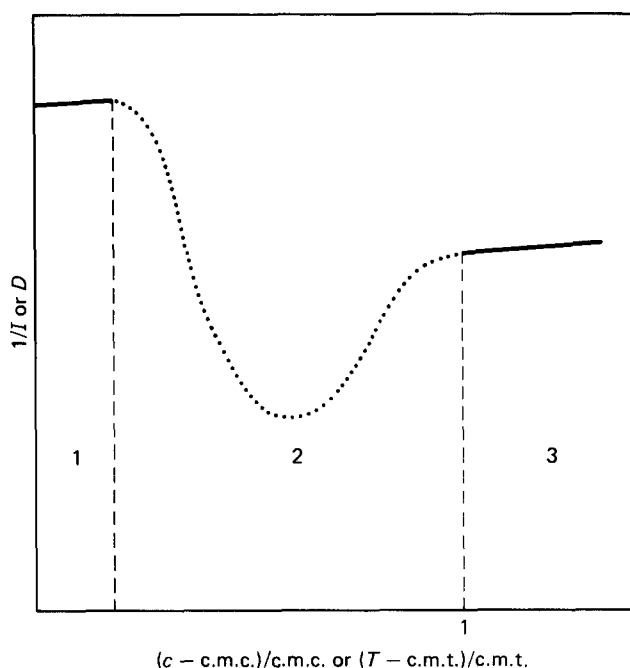


Figure 10 Schematic variation of $1/I$ or D as a function of $(c - \text{c.m.c.})/\text{c.m.c.}$ or $(T - \text{c.m.t.})/\text{c.m.t.}$: region 1, dilute solution of monomers; region 2, region of 'anomalous micellization effect'; region 3, micellar solutions

The anomalous micellization effect is not yet well understood. It is a major effect observed in 1-chloro-*n*-hexane solutions at high temperature. In contrast, this effect is minimized in 1-chloro-*n*-hexane/dioxane mixtures and can be detected through the concentration dependence of c/I or D ($\phi = 0.90$, $T = 46.1$ and 37.2°C on Figure 5; $\phi = 0.90$, $T = 32.6^\circ\text{C}$ on Figure 8). As interpreted by other authors¹⁰⁻¹² it could correspond to the presence of large ellipsoidal structures formed by linear associations of a small number of copolymer molecules. The small amount of good solvent for both PMMA and PS sequences in 1-chloro-*n*-hexane/dioxane mixtures curtails the domain where this effect takes place compared to pure 1-chloro-*n*-hexane solutions.

REFERENCES

- 1 Duval, M. and Picot, C. *Polymer* 1987, **28**, 793
- 2 Elias, H. G. in 'Light Scattering from Polymer Solutions', (Ed. M. B. Huglin), Academic Press, London, 1972, Chap. 9
- 3 Strazielle, C. in 'Light Scattering from Polymer Solutions', (Ed. M. B. Huglin), Academic Press, London, 1972, Chap. 9
- 4 Duval, M. and Coles, H. J. *Rev. Phys. Appl.* 1980, **15**, 1399
- 5 Duval, M., François, J. and Sarazin, D. *Polymer* 1985, **26**, 397
- 6 Sikora, A. and Tuzar, Z. *Makromol. Chem.* 1983, **184**, 2049
- 7 Mandema, W., Emeis, C. A. and Zeldenrust, H. *Makromol. Chem.* 1979, **180**, 2163
- 8 Mandema, W., Zeldenrust, H. and Emeis, C. A. *Makromol. Chem.* 1979, **180**, 1521
- 9 Kotaka, T., Tanaka, T. and Inagaki, H. *Polym. J.* 1972, **3**, 327
- 10 Tuzar, Z., Stepanek, P., Konak, C. and Kratochvil, P. *J. Colloid Interface Sci.* 1985, **105**, 372
- 11 Lally, T. P. and Price, C. *Polymer* 1974, **15**, 325
- 12 Tuzar, Z., Sikora, A., Petrus, V. and Kratochvil, P. *Makromol. Chem.* 1977, **178**, 2743